



## Performance of WRF for Simulation of Mesoscale Meteorological Characteristics for Air Quality Assessment over Tropical Coastal City, Chennai

SRIKANTH MADALA,<sup>1</sup> C. V. SRINIVAS,<sup>2</sup> and A. N. V. SATYANARAYANA<sup>3</sup>

**Abstract**—The land–sea breezes (LSBs) play an important role in transporting air pollution from urban areas on the coast. In this study, the Advanced Research WRF (ARW) mesoscale model is used for predicting boundary layer features to understand the transport of pollution in different seasons over the coastal region of Chennai in Southern India. Sensitivity experiments are conducted with two non-local [Yonsei University (YSU) and Asymmetric Convective Model version 2 (ACM2)] and three turbulence kinetic energy (TKE) closure [Mellor–Yamada–Nakanishi and Niino Level 2.5 (MYNN2) and Mellor–Yamada–Janjic (MYJ) and quasi-normal scale elimination (QNSE)], planetary boundary layer (PBL) parameterization schemes for simulating the thermodynamic structure, and low-level atmospheric flow in different seasons. Comparison of simulations with observations from a global positioning system (GPS) radiosonde, meteorological tower, automated weather stations, and Doppler weather radar (DWR)-derived wind data reveals that the characteristics of LSBs vary widely in different seasons and are more prominent during the pre-monsoon and monsoon seasons (March–September) with large horizontal and vertical extents compared to the post-monsoon and winter seasons. The qualitative and quantitative results indicate that simulations with ACM2 followed by MYNN2 and YSU produced various features of the LSBs, boundary layer parameters and the thermodynamical structure in better agreement with observations than other tested physical parameterization schemes. Simulations revealed seasonal variation of onset time, vertical extent of LSBs, and mixed layer depth, which would influence the air pollution dispersion in different seasons over the study region.

**Key words:** ARW model, land–sea breezes, planetary boundary layer, air pollution.

### 1. Introduction

The meteorological conditions, convection, local climate, and air quality in coastal areas are influenced by the thermally driven land–sea-breeze (LSB)-type mesoscale systems (Suresh 2007). The sea-breeze circulations cause air pollution impacts in urban coastal regions by transporting the air pollutants from nearby emission sources (Bouchlaghem et al. 2007) and marine pollutants to the inland areas (Reche et al. 2011). The LSBs are a thermally generated mesoscale circulation due to land–sea differential heating and associated low-level pressure gradient in the atmosphere. These systems follow a clear diurnal cycle and re-circulate the emissions from local sources to the land areas. The LSBs are studied both observationally and numerically over various regions including tropical Indian coasts (Lasry et al. 2005; Li et al. 2013; Luhar and Hurley 2003; Mahrer and Pielke 1977; Melas et al. 1995; Simpson et al. 2007; Suresh 2007; Srinivas et al. 2007, 2015) to understand their implications in air pollution transport and local weather.

Regional meteorological factors such as low-level atmospheric circulation, atmospheric moisture, atmospheric stability conditions, mixed layer heights, mountain–valley flows and LSBs, etc., influence the air pollution dispersion and air quality (Panda et al. 2009; Panda and Sharan 2012; Seaman 2000; Srinivas et al. 2007; Madala et al. 2015a, b). The sea breeze in tropical coastal regions is particularly interesting due to strong daytime heating and resulting intensive low-level circulations that influence air pollution transport as well as local convection (Liu and Chan 2002). The sea-breeze characteristics such as timing, intensity, its dynamics, and horizontal

---

**Electronic supplementary material** The online version of this article (doi:10.1007/s00024-017-1662-3) contains supplementary material, which is available to authorized users.

---

<sup>1</sup> Centre for Remote Imaging Sensing and Processing, National University of Singapore, Singapore, Singapore.

<sup>2</sup> Radiological Safety Division, Health, Safety and Environment Group, Indira Gandhi Centre for Atomic Research, Homi Bhabha National Institute, Kalpakkam 603102, India. E-mail: venkatasrinivasc@yahoo.com; cvsri@igcar.gov.in

<sup>3</sup> Centre for Oceans, Rivers, Atmosphere and Land Sciences, Indian Institute of Technology Kharagpur, Kharagpur 721302, India.

extents may be influenced by the urban environments near the coast due to heat island effects and interaction of sea breeze front with urban features (Joseph et al. 2008; Li et al. 2013; Yoshikado 1994; Ohashi and Kida 2002).

Chennai city (13°04'N, 80°17'E) situated in the southeast coast of India has plain topography (6 m above mean sea level) and is the capital of Tamilnadu. The city frequently experiences sea-breeze circulation due to intense heating and large land–sea temperature gradients. The city has many pollutant sources such as power plants, industries as well as large mobile pollution and various anthropogenic activities (Jayanthi and Krishnamoorthy 2006; Srimuruganandam and Shiva Nagendra 2011; Thilagaraj et al. 2014). Srinivas et al. (2006, 2007) using MM5 mesoscale model for a rural area Kalpakkam south of Chennai on the southeast coast showed that the characteristics of sea breeze and coastal boundary layer vary in different seasons according to the prevailing large-scale winds and surface fluxes. Observational analysis on the sea-breeze events along the east coast around Chennai (Simpson et al. 2007) indicates sea-breeze circulation occurs for over 70–80% of time in the summer months and it is the main mechanism responsible for most of the convective rainfall during summer monsoon over this region. Venkatesan et al. (2009) using a simple mesoscale model showed that significant changes occur in the surface meteorological variables and low-level circulation over Chennai as a result of sea breezes in the pre-monsoon period. Doppler weather radar (DWR) observations over Chennai city indicate that the frequency of sea breeze in Chennai is greater during the southwest monsoon season (June–September) and sea breeze extends in majority of the cases up to 50-km inland with the mean depth of the circulation varying between 300 and 1000 m (Suresh 2007). In addition, mini-SODAR observations at a nearby station Kalpakkam indicate typical onshore vertical winds of 2.0–2.5 ms<sup>-1</sup> (Prabha et al. 2002). The above review shows that studies on sea breeze over Chennai region are limited to summer season and it is required to analyze the boundary layer wind field in various seasons to understand the role of synoptic flow on the sea-breeze characteristics for impact on air pollution transport. Furthermore, the

modeling studies on LSBs over Chennai city are limited to few cases and do not offer comparison with vertical observations such as DWR data, which is advantageous in analyzing the sea breeze and associated mesoscale flow systems (Ruscher et al. 1995) for validation. In the present study, an attempt is made to study the performance of ARW mesoscale model to simulate the seasonal characteristics of LSBs over the Chennai city and validate the features with various surface and upper air observations including DWR data. The characteristics of mesoscale wind field, coastal boundary layer in and around Chennai in different seasons under various synoptic flow are analyzed from model simulations. This paper is organized as follows. In Sect. 2, we provide the details of data used and methodology for numerical simulations. Results of numerical experiments are presented in Sect. 3 and Sect. 4 provides the main conclusions of the study.

## 2. Data and Methodology

### 2.1. Data

In the present study, several sources of observations are used for model validation. They comprise data from 50-m micrometeorological tower situated at Sathyabama University, Chennai, 12 automated weather stations (IIT, Chennai, MC ENG. Magaral, Chennai, JEC Thiruninaravur, Chinna Semavaram Ponneri, Ponneri thaluk office road, Vellammal, Red Hills, Cholavaram, Tamapakkam, Koduvalli, Air Force Station Tambaram and MSSRF Taramani, Chennai) of Indian Space Research Organization, DWR data on winds from Cyclone Detection Radar (CDR) Station, India Meteorological Department (IMD), Chennai, India, and one daily upper air radiosonde observations of IMD, Chennai. The measured parameters from the 50-m tower are air temperature (AT) (°C), relative humidity (RH) (%), wind speed (WS) (ms<sup>-1</sup>), and wind direction (WD) (°) at five different heights, 2, 8, 16, 32, and 50 m. The data from automated weather station consist of AT, RH, WS, and WD downloaded from Meteorological and Oceanographic Satellite Data Archival Centre (MOSDAC) (<http://www.mosdac.gov.in>). The horizontal winds at different heights derived from

DWR, Chennai are used for comparison of simulated winds.

## 2.2. Model Configuration and Experiment Design

The ARW (Version 3.2) 3D non-hydrostatic mesoscale model is used in the present study. The model consists of Eulerian mass solver with fully compressible non-hydrostatic equations, terrain following vertical coordinate and staggered horizontal grid with complete Coriolis and curvature terms (Skamarock et al. 2008).

To study the role of synoptic flow in the development of sea-breeze circulation, simulations are performed for 8 days characterized with fair weather in different seasons. The selected dates for simulations are 21–29 January 2011 representing winter season, 06–14 April 2011 representing pre-monsoon season, 03–07 and 12–16 August 2011 representing monsoon season, and 07–15 November 2011 representing post-monsoon season as per availability of observations for model validation.

The ARW model is designed with 3 nested domains with grid resolutions of 27, 9, and 3 km and 51 unequally spaced vertical eta levels and the

model top is fixed at 50 hPa. The outer domain (d01) covers a larger region with 27-km resolution and  $60 \times 61$  grids, second inner domain (d02) has 9-km resolution with  $100 \times 100$  grids, and innermost domain (d03) has 3-km resolution with  $121 \times 121$  grids (Fig. 1a). The second and third nests are two-way interactive domains. The initial and boundary conditions are derived from 6 hourly,  $1^\circ \times 1^\circ$  resolution National Centres for Environmental Prediction (NCEP) FNL data. The United States Geological Survey (USGS) topography and vegetation data (25 categories) and Food and Agriculture Organization of the United Nations (FAO) Soils data (17 categories) with resolutions 5, 2 m, and 30 s (0.925 km) available as part of WRF data library are used to define the lower boundary conditions. The spatial terrain elevation in the inner third domain is shown in Fig. 1b. The model is initialized at 0000 UTC and integrated for a period of 48 h in all the simulations starting on 21, 23, 25, and 27 January 2011 for winter season, 06, 08, 10, and 12 April 2011 for pre-monsoon season, 03, 05, 12, and 14 August 2011 for monsoon season, and 07, 09, 11, and 13 November 2011 for post-monsoon season. The first 6-h period is considered for model-spin up for each simulation.

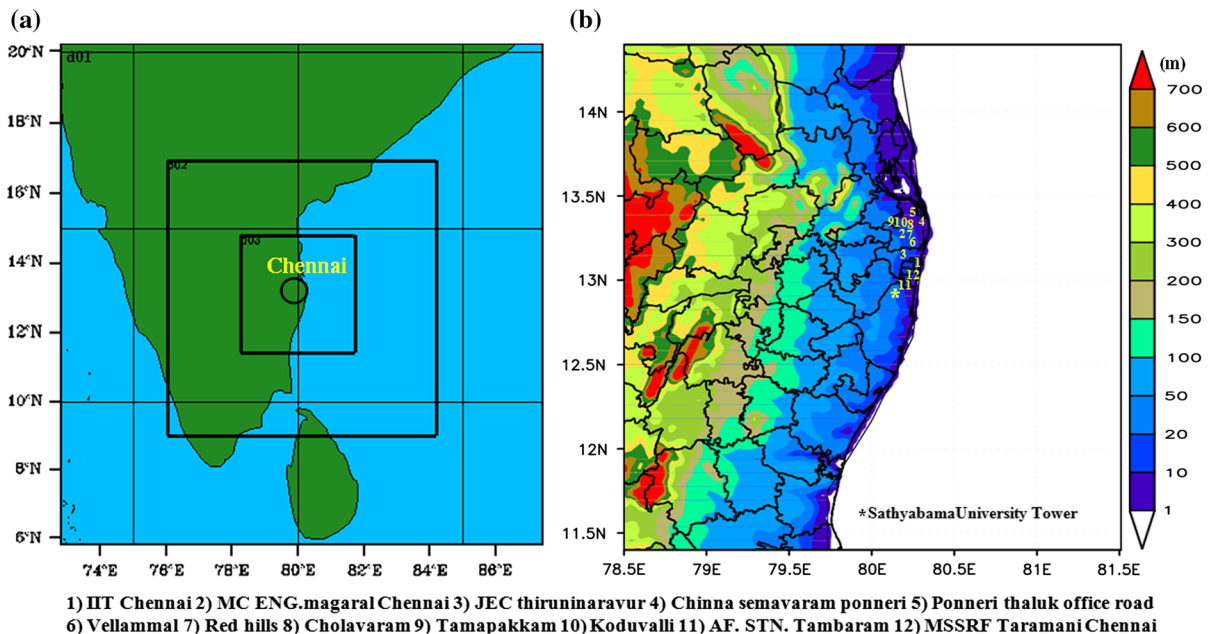


Figure 1  
Domains used in the ARW model

### 2.3. Sensitivity Experiments

In numerical models, the planetary boundary layer (PBL) and land-surface processes influence the characteristics of LSBs by affecting the land-sea temperatures and the surface fluxes (Hariprasad et al. 2014; Panda and Sharan 2012; Perez et al. 2006; Prtenjak and Grisogono 2002; Srinivas et al. 2007, DWR, Chennai are compared with model simulations). Hence, in the present study, sensitivity experiments are conducted with different PBL physics, namely, two non-local schemes [Yonsei University (YSU) and Asymmetric Convective Model version 2 (ACM2)] and three local turbulence kinetic energy (TKE) closure [Mellor–Yamada–Nakanishi and Niino Level 2.5 (MYNN2), Mellor–Yamada–Janjic (MYJ), and quasi-normal scale elimination (QNSE)]. In the local-closure schemes (MYJ, MYNN2, and QNSE), the turbulent fluxes are derived from known quantities or their vertical derivatives at the same grid point. In contrast, the non-local-closure schemes (YSU and ACM2) relate the turbulence fluxes to known quantities at any number of grid points elsewhere in the vertical. The YSU and ACM2 use first-order closure following the gradient transport K theory, where the second moments are parameterized. In the higher order local diffusion schemes (MYJ, MYNN2, and QNSE), eddy diffusivity coefficients for momentum and heat are parameterized through the predicted turbulence kinetic energy (TKE) and a non-dimensional stability function. In the non-local diffusion schemes (YSU and ACM2), a correction term called ‘counter gradient flux’ to represent effects of large-scale eddies is applied in the diffusion equations. The empirical formulations of the PBL schemes are described elsewhere (e.g., Skamarock et al. 2008; Shin and Hong 2011; Xie et al. 2012; Madala et al. 2014; Hariprasad et al. 2014).

### 2.4. Model Validation and Statistical Evaluation

Simulated surface meteorological variables are compared against observations of AT, RH at 2 m, and WS, WD at 10 m above ground level (AGL) measured at Sathyabama University tower and 12 automated weather stations. The vertical profiles of wind, relative humidity, and potential temperature

during the study period are validated with daily upper air radiosonde observation of IMD, Chennai. The model time–height section of horizontal wind and vertical extent of sea breeze are compared with DWR data at CDR station, IMD, Chennai. The model variables are extracted from the nearest grid points to observation locations used for comparisons. Results are compared both qualitatively and quantitatively following standard procedures. The quantitative performance is assessed by computing error statistics such as mean bias (MB), mean absolute error (MAE), root mean square error (RMSE), and correlation coefficient (CC) between model outputs and observations.

## 3. Results and Discussion

The simulations of 8 days in each season are analyzed. Typical results of temporal and spatial variation in the flow field, vertical structure of the horizontal circulation, boundary layer height and diurnal variation in the surface meteorological parameters as well as thermo-dynamical structure of the lower atmosphere on few representative days are discussed below. The results are shown mostly from the simulation ACM2 for non-local PBL schemes (YSU and ACM2) and MYNN2 for local diffusion schemes (QNSE, MYJ, and MYNN2) due to small differences in results among these classes of PBL schemes.

### 3.1. Simulated Boundary Layer Flow Field in Different Seasons

The flow field characteristics at Chennai are diurnally and seasonally variable as evident from the following discussion. The spatial wind field, temperature as well as PBL height (PBLH) are examined from the high-resolution inner most domain (d03) to analyze the timing, horizontal, and vertical extents of LSB circulations in and around Chennai in different seasons. The simulation on typical winter day 24 January 2011 indicated prevalence of land breeze in the morning at 0100 UTC (0630 IST) and sea breeze in the afternoon at 0800 UTC (1330 IST), respectively (figures not shown).



The background flow in the winter case (24 January 2011) is northerly. The simulation at 0800 UTC (1330 IST) (in the afternoon) shows prevalence of sea breeze all over the domain along with formation of a shallow thermal internal boundary layer (TIBL) at the coast (Gryning and Batchvarova 1990) in all the simulations (figure not shown). The horizontal wind observations from DWR, Chennai are compared with model simulations shown in Figs. 2a, b and 7a, b, respectively (0000–2330 UTC on 24 January 2011 for winter season, 0000–2330 UTC on 13 April 2011 for pre-monsoon season, 0000–2330 UTC on 13 August 2011 for monsoon season, and 0000–2330 UTC on 10 November 2011 for post-monsoon season). The extent of the mesoscale circulations is examined from the vertical section of DWR-derived

horizontal winds at different levels in the atmosphere up to 2.4 km. For the winter case (24 January 2011), it is seen that the winds above 1.5 km above ground level (AGL) are easterly and the winds below 1.5 km turn to be north-northeasterly representing boundary layer shear. A small diurnal variation of winds is seen in the lower 0–500-m layer. The flow in this layer is seen to be northerly during stable morning hours, north-northeasterly from 0100 to 0700 UTC (0630–1230 IST) and then turn as strong northeasterly ( $\sim 8 \text{ ms}^{-1}$ ) indicating sea-breeze regime until 1200 UTC (1730 IST). The flow in the 0–500-m layer changes as east-northeasterly after 1200 UTC (1730 IST) and then finally changes as northerly by 1600 UTC (2130 IST) indicating the changeover as large-scale winds. Thus, the DWR wind observations show

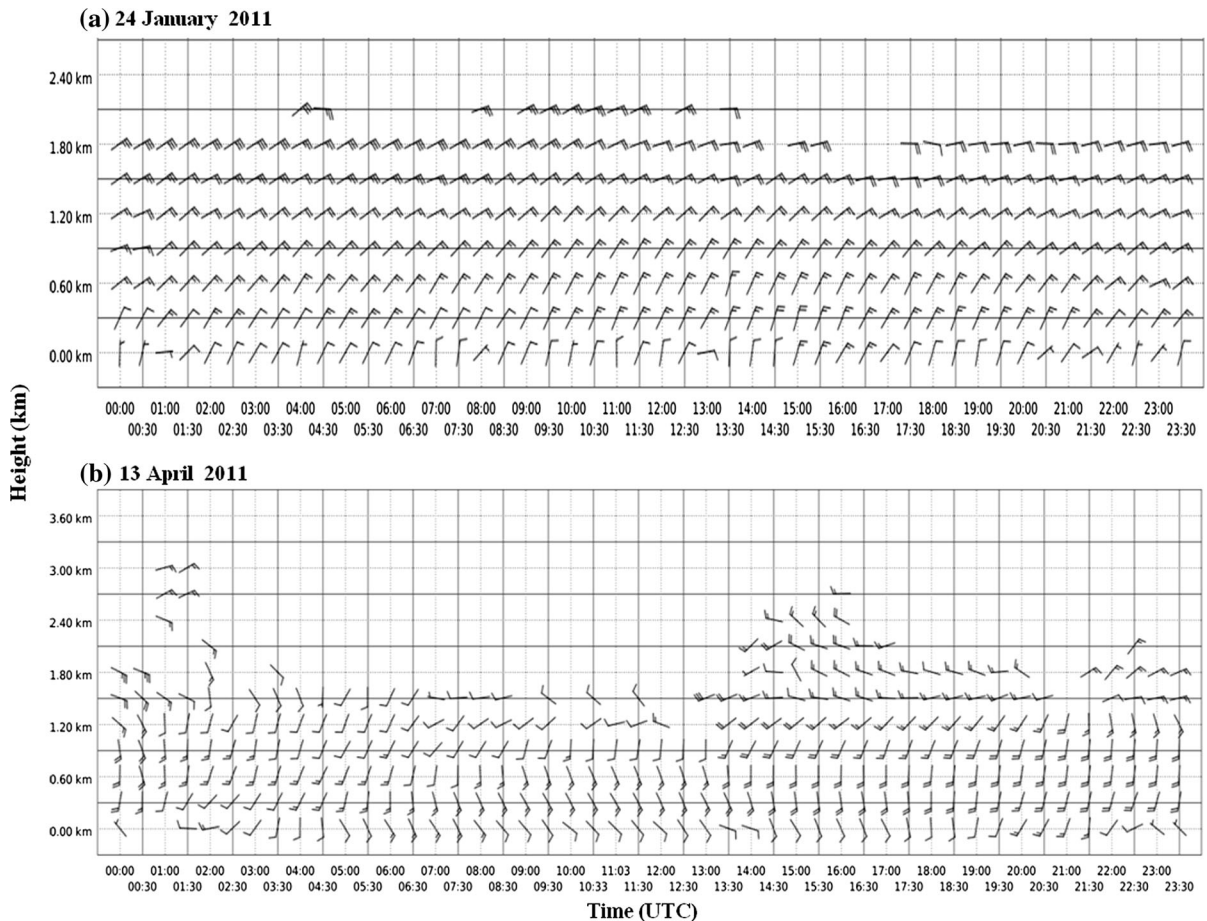


Figure 2

Time–height section of horizontal wind estimated from DWR at CDR station, IMD, Chennai during **a** 0000–2330 UTC on 24 January 2011 for winter case and **b** 0000–2330 UTC on 13 April 2011 for pre-monsoon case

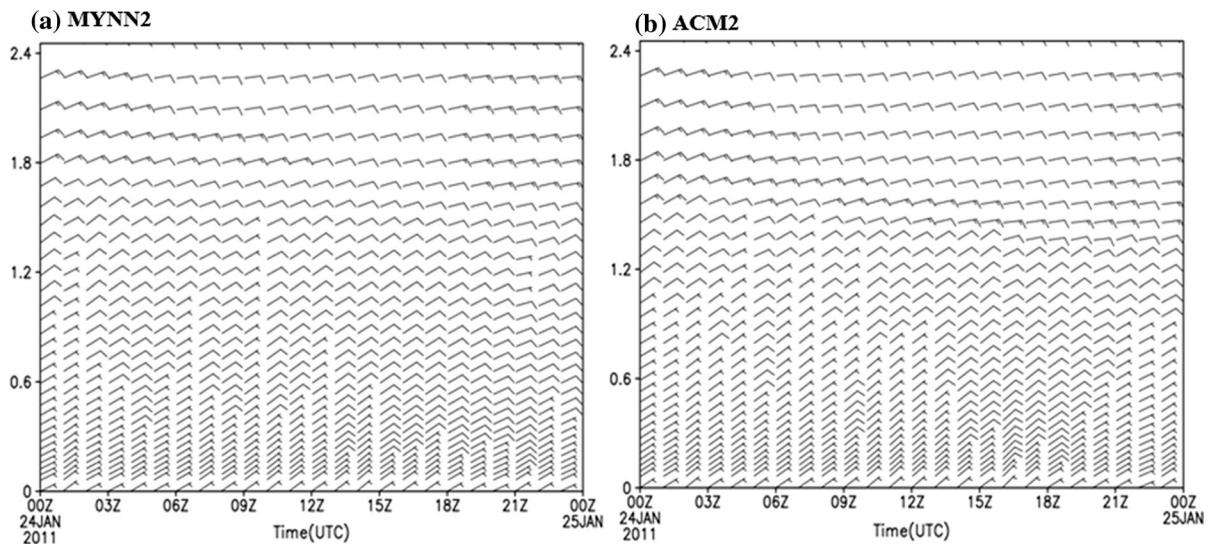


Figure 3

Time–height section of simulated horizontal winds corresponding to CDR station, IMD, Chennai during 0000–2330 UTC on 24 January 2011 for winter case

the occurrence of sea breeze 0700–1200 UTC (1230–1730 IST) as northeasterly winds during the winter case. The time–height section of WRF simulated winds for 24 January 2011 (winter season) (Fig. 3) indicates that the wind shear in the lower 2.4-km layer is well-represented in simulations with different PBL physics cases. The mesoscale flow extends vertically to 1.2 km in YSU and ACM2; 0.9 km in QNSE and MYJ, and 0.4 km in MYNN2 indicating simulation of deep cells of sea-breeze circulations with non-local mixing schemes (YSU and ACM2) similar to Srinivas et al. (2015). The diurnal flow variation in the lowest 500-m layer is simulated in good agreement with DWR-observed winds in all the five PBL physics.

Simulated flow field for a typical day 13 April 2011 in the pre-monsoon season (figure not shown) indicated land breeze comprising calm westerly winds in the southern and central parts and moderate southwesterly flow in the northern parts in the morning time (0100 UTC/0630 IST). All the simulations show the development of southeasterly mesoscale sea-breeze circulation at 0600 UTC (1130 IST) (Fig. 4), indicating early onset of sea breeze by  $\approx 1\frac{1}{2}$  h in summer compared to winter case. The sea breeze covers entire domain by 0600 UTC (1130 IST) in YSU, MYNN2, and ACM2, while

it is confined to  $\approx 20$  km from the coast in QNSE and MYJ. A few differences in simulated flow field in different PBL cases are due to the variation in the eddy diffusivities and the resulting differences in winds. The winds are stronger in the simulations YSU, QNSE, and MYNN2 compared to MYJ and ACM2. This suggests that the pollutant plumes would be transported more rapidly leading to lesser pollutant concentrations when meteorological fields are used from simulations with YSU, QNSE, and MYNN2 as reported in recent studies (Madala et al. 2016). In all the simulations, calm winds are noticed in the land areas before the sea breeze extends inland (not shown). The calm winds lead to poor dispersion of air pollutants and cause stagnation resulting in high ground-level concentration of pollutants (Goyal and Rama Krishna 2002; Sharan et al. 1995). The sea breeze extended all over the domain by 0800 UTC (1330 IST) in all simulations (figure not shown). In the daytime at 0600 UTC (1130 IST), deep-mixed layers ( $\approx 1300$  m) are simulated in all the PBL schemes except QNSE which produced very deep boundary layers ( $\approx 1800$  m) (Fig. 4). Along the coast relatively shallow boundary layers (250–750 m) indicating formation of TIBL simulated in all the PBL schemes. The mixed layer over land region has grown to 2000 m in all the PBL schemes except

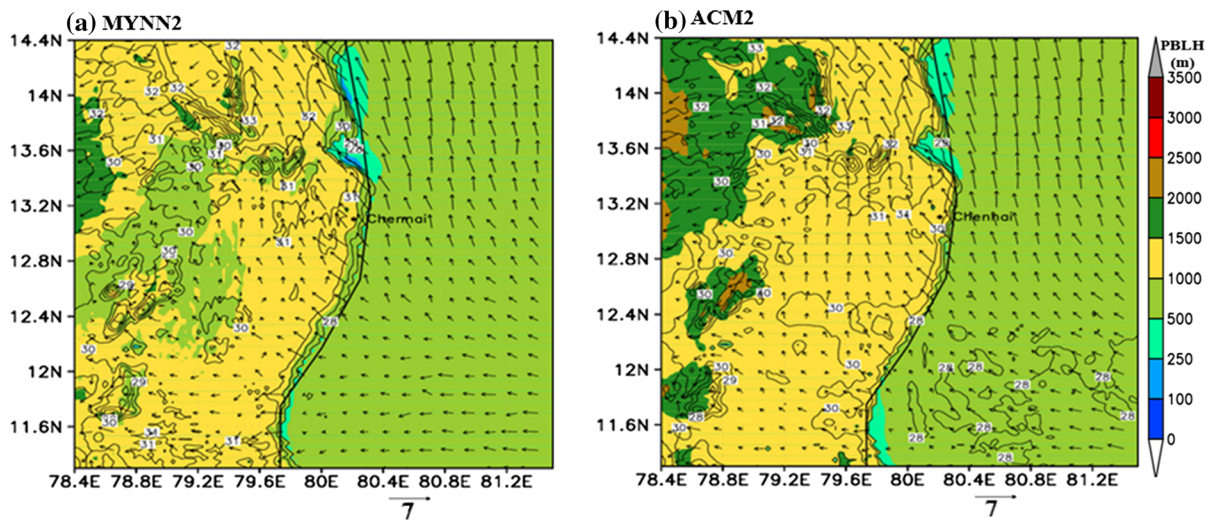


Figure 4

Simulated surface-level wind vectors, temperature, and planetary boundary layer (PBL) height for inner most domain (d03) on 13 April 2011 (pre-monsoon case) at 0600 UTC (sea-breeze onset) from simulations with different PBL schemes

QNSE, which produced a very deep-mixed layer (2700 m). The time–height section of Doppler radar wind observations on 13 April 2011 (Fig. 2b) shows the large-scale easterly winds above 1.2-km AGL throughout the day. In the lower 1-km region, the winds exhibit significant shear as well as large diurnal variability of flow in agreement with earlier studies at the southeast coast (Srinivas et al. 2007). In the lower 500-m layer, the winds are westerly in the morning until 0200 UTC (0730 IST), southwesterly until 0300 UTC (0830 IST), and southerly from 0330 UTC (0900 IST). The winds become strong ( $\sim 8 \text{ ms}^{-1}$ ) and turn as southeasterly from 0500 UTC (1030 IST) to 1400 UTC (1930 IST) indicating the development of sea-breeze circulation. Thereafter, the flow changes as southerly until 2130 UTC (0400 IST) and then from 2230 UTC (0500 IST) onwards as westerly and northwesterly indicating land breeze. The DWR wind observations show the mesoscale circulations to extend up to 1000 m vertically in the boundary layer, where pollution dispersion occurs. The strength, inland, and vertical extents of such mesoscale flows determine the air quality in the coastal areas. The time–height section of model simulated horizontal winds for 13 April 2011 (pre-monsoon season) (Fig. 5) shows the northwesterly/southwesterly winds in the morning time and development of mesoscale southeasterly sea breeze in

the daytime which is slightly different in different PBL schemes. These local circulations cause impact in the downwind areas in the northwestern, northern and northeastern sectors by transporting effluent releases from tall industrial stacks in summer (Madala et al. 2016). The onset of sea breeze is little early (i.e., from 0500 UTC/1030 IST) in ACM2, YSU, and MYNN2 and delayed by 1 h in the cases QNSE and MYJ. Furthermore, large shear in the boundary layer winds is noticed in the simulations with higher order turbulence closure physics QNSE, MYJ, and MYNN2 as compared to the non-local first-order closures YSU and ACM2, indicating stronger shear turbulence and hence larger dispersion in the former (Madala et al. 2016).

The synoptic winds in the study domain on a typical day 13 August 2011 in southwest monsoon season are strong westerly/southwesterly. The southwesterly winds offer strong opposing force to the mesoscale sea-breeze winds and lead to either suppression or late onset of sea breeze in this season (Srinivas et al. 2005). However, the opposing synoptic winds produce intense sea-breeze fronts due to strong convergence in the lower levels leading to convection (Srinivas et al. 2006, 2007). The simulated low-level flow field in the daytime at 1000 UTC (1530 IST) indicates strong ( $\sim 6 \text{ ms}^{-1}$ ) westerly winds over the land areas and the incidence of



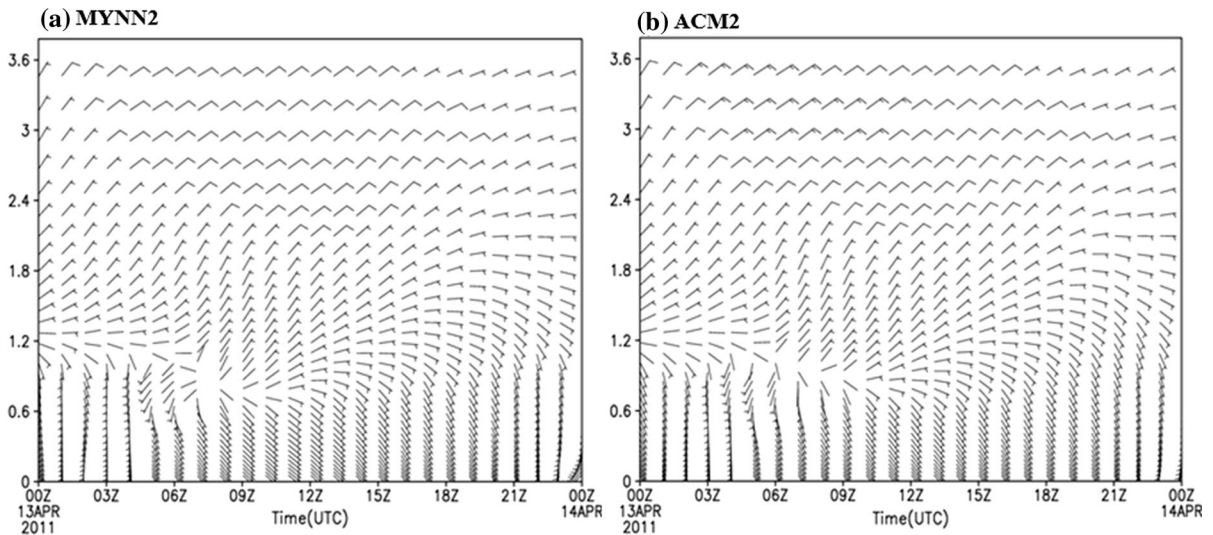


Figure 5

Time–height section of simulated horizontal wind corresponding to CDR station, IMD, Chennai during 0000–2330 UTC on 13 April 2011 for pre-monsoon case

southeasterly onshore winds at the coast (not shown). Simulated flow fields from experiments with different PBL physics for afternoon on 13 August are shown in Fig. 6. Onset of sea breeze is seen at 1000 UTC (1530 IST), indicating that a delay of about 4 h in sea-breeze onset compared to summer season and the inland extent of sea breeze are confined to a small fetch (~20 km) across the coast (Fig. 6). A complete development of sea breeze extending to about 50 km

across the coast is noticed at 1300 UTC (1830 IST) (figure not shown). The inland extent of sea breeze differently simulated in different PBL physics. Both non-local schemes (YSU and ACM2) predicted the sea breeze to prevail up to 35–45 km across the coast, while the TKE closures (QNSE, MYNN2, and MYJ) simulated the inland extent as 45–60 km. A shallow boundary layer indicating formation of TIBL (Gryning and Batchvarova 1990) is seen near the coast.

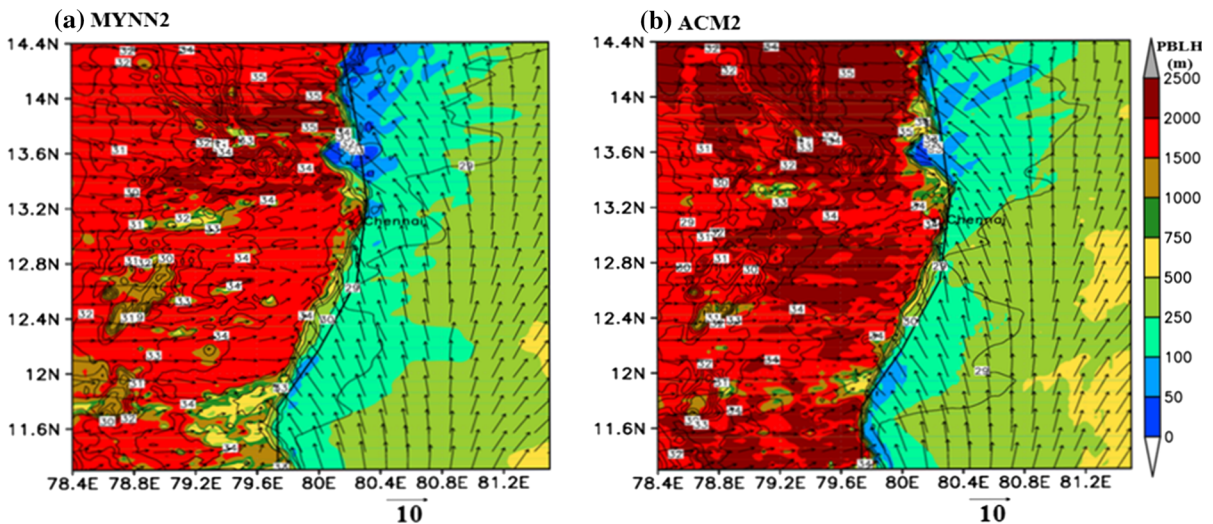


Figure 6

Simulated surface-level wind vectors, temperature and planetary boundary layer height for inner most domain (d3) at on 13 August 2011 (monsoon case) at 1000 UTC (sea-breeze onset) from simulations with different PBL schemes a MYNN2 and b ACM2

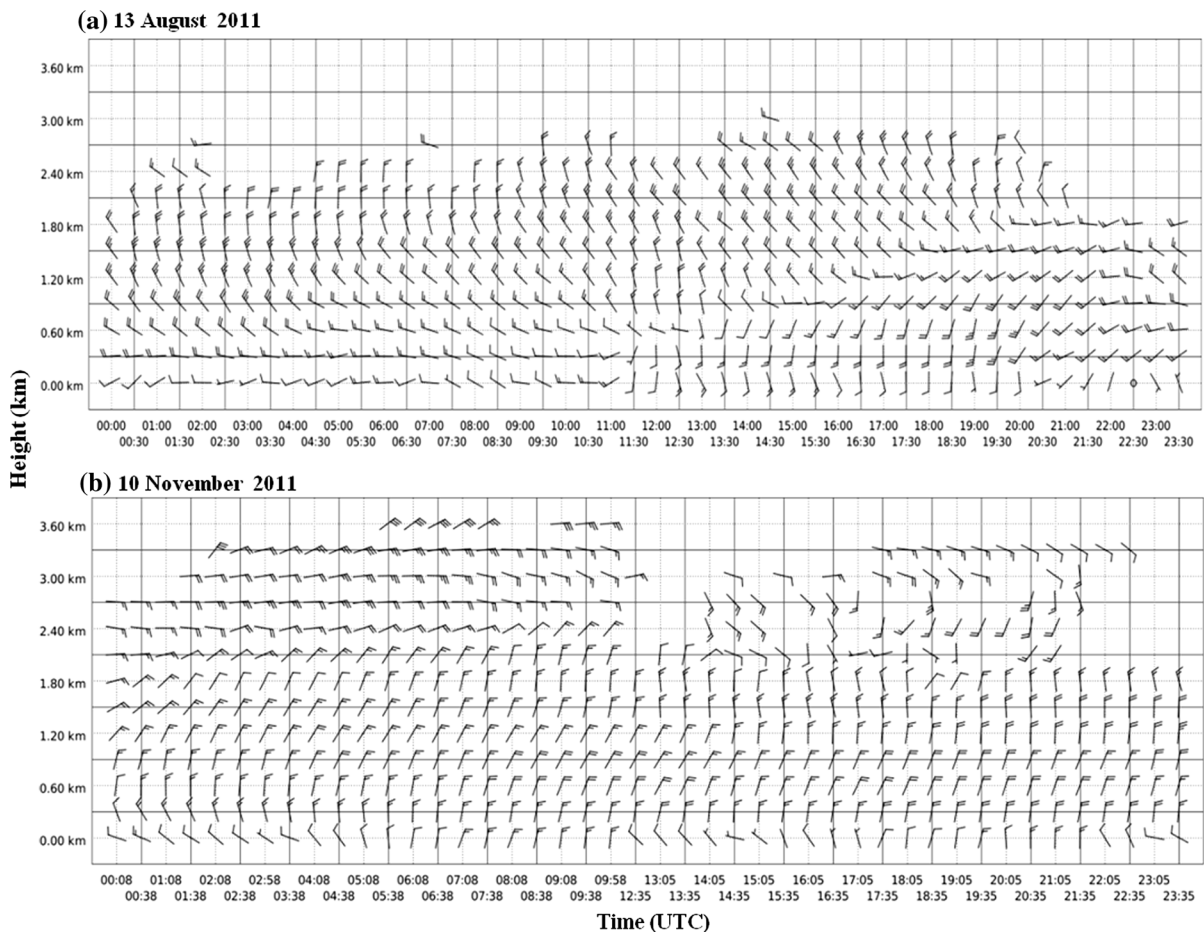


Figure 7

Time–height section of horizontal wind estimated from DWR at CDR station, IMD, Chennai during **a** 0000–2330 UTC on 13 August 2011 for monsoon case and **b** 0000–2330 UTC 10 November 2011 for post-monsoon case

While MYNN2, YSU, ACM2, and MYJ predicted a shallow TIBL (100–250 m), the QNSE predicted relatively deep coastal boundary layer ( $\sim 750$  m) in agreement with the results at Kalpakkam coast (Hariprasad et al. 2014).

The time–height section of DWR-derived horizontal winds on 13 August 2011 (monsoon season) at Chennai shows northerly and northwesterly winds above 2-km AGL (Fig. 7a). The winds in the lower 500-m layer are noted to be westerly from 0000 UTC (0530 IST) to 1000 UTC (1530 IST). Subsequently, southerly and southeasterly sea breeze prevailed until 1900 UTC (0030 IST). The vertical section of simulated horizontal winds for 13 August 2011 (figure not shown) shows an early onset of sea breeze confined to a very shallow layer of about 800 m in all

PBL schemes. There are some differences especially in the layer above 600 m in which the observations indicated northerly winds, while the model predicted westerly component. Under these diurnally varying flows, the pollutant plumes would be transported to north, northeast, and eastern sectors in monsoon case (Madala et al. 2016).

In the case of post-monsoon season (10 November 2011), the simulated morning time winds are noticed to be northwesterly (figure not shown) in all the PBL physics cases and associated with very shallow stable boundary layers ( $\sim 150$  m). During daytime at 0500 UTC (1030 IST), the low-level winds turn to be northerly in the eastern parts and north-northeasterly in the western parts, and subsequently, the winds turn as northeasterly in all the simulations (figure not shown).



However, these northeasterly winds represent synoptic scale flow in this post-monsoon season. These features are well-supported by the DWR-derived horizontal winds (Fig. 7b). The observed DWR winds are most of the time northerly with small diurnal variation in flow above 300-m AGL (Fig. 7b). In the lowest 300-m layer, the winds are noted to be westerly/northwesterly from 0000 UTC (0530 IST) to 0500 UTC (1030 IST). Subsequently, the winds change as northerly until 1000 UTC (1530 IST) and then as north-northeasterly until 1200 UTC (1730 IST) indicating modest diurnal variation of winds in the lower boundary layer during the post-monsoon season. The above features agree well with the DWR wind observations (Fig. 7). The land-breeze regime is simulated as 8 h [from 1900 UTC (0030 IST) to 0300 UTC (0830 IST)] with YSU, QNSE, MYNN2, and ACM2 and as 6 h [from 2300 UTC (0430 IST) to 0300 UTC (0830 IST)] with MYJ scheme. This indicates that that the pollutant plumes in Chennai would be transported to southwest sector in the post-monsoon season as also recently reported by Madala et al. (2016). Relatively stronger dispersion is expected in the cases YSU and ACM2 due to stronger winds.

The characteristics of LSB circulations simulated by ARW in different seasons with different PBL schemes are presented in Table 1. Observations and simulations both indicate (Table 1) longer duration of sea breeze during pre-monsoon ( $\sim 12$  h) followed by

monsoon ( $\sim 6$  h) and post-monsoon ( $\sim 3$  h). In winter, the sea breeze merges with the synoptic flow and the exact duration is not well-defined. The sea breeze prevails for  $\sim 5$ – $6$  h during monsoon depending on the large-scale flow, cloud cover, and the land-surface heating (Srinivas et al. 2006). All the simulations indicate an early onset of sea breeze in pre-monsoon (0400 UTC/0930 IST) followed by monsoon (0800 UTC/1330 IST). The sea breeze extends vertically up to  $\sim 900$  m in pre-monsoon,  $\sim 800$  m in monsoon, and  $\sim 400$  m in post-monsoon season. The YSU, ACM2, and MYNN2 simulate early onset, longer duration, and more intensity with deeper sea-breeze cells in all the seasons, respectively. These circulation features suggest widely varying pollutant dispersion patterns in Chennai in different seasons (Madala et al. 2016).

### 3.2. Flow Field Across the Coast

The vertical section of the circulation ( $U$  and  $W$  wind vectors) and potential temperature in the boundary layer along the Chennai city latitude ( $13^\circ\text{N}$ ) and across land and sea from  $79.8^\circ\text{E}$  to  $80.8^\circ\text{E}$  at day time 0700 UTC (1230 IST) is analyzed from the high-resolution inner most domain (d03) on 13 April 2011 (Fig. 8) for pre-monsoon case, where the sea breeze is developed more predominantly. Variations in the wind field and potential temperature

Table 1

*Results of simulation in different cases of PBL parameterisation schemes for all seasons*

Season	Parameter	Observation	YSU	QNSE	MYNN2	MYJ	ACM2
Winter	Sea-breeze onset (UTC)	0700	0600	0600	0600	0500	0600
	Duration of sea breeze (UTC)	0700–1700	0600–1800	0600–1800	0600–1700	0500–1700	0600–1700
	Vertical extent of sea breeze (m)	Not clear	Not clear	Not clear	Not clear	Not clear	Not clear
	Intensity of sea breeze ( $\text{ms}^{-1}$ )	4	4.6	7.5	5.2	6.8	5
Pre-monsoon	Sea-breeze onset (UTC)	0500	0500	0600	0500	0500	0400
	Duration of sea breeze (UTC)	0500–1700	0500–1700	0600–1600	0500–1600	0500–1600	0400–1700
	Vertical extent of sea breeze (m)	900	900	1000	800	800	800
	Intensity of sea breeze ( $\text{ms}^{-1}$ )	4.2	5.0	6.2	5.0	6.0	5.0
Monsoon	Sea-breeze onset (UTC)	1000	0900	0900	0900	0900	0900
	Duration of sea breeze (UTC)	1000–1700	0900–1700	0900–1700	0900–1700	0700–1700	0700–1700
	Vertical extent of sea breeze (m)	800	700	500	600	500	800
	Intensity of sea breeze ( $\text{ms}^{-1}$ )	5.5	3.8	5.8	3.8	5.5	3.9
Post-monsoon	Sea-breeze onset (UTC)	0800	0600	0700	0600	0700	0600
	Duration of sea breeze (UTC)	0800–1200	0600–1200	0700–1400	0600–1400	0700–1400	0600–1400
	Vertical extent of sea breeze (m)	400	500	500	600	600	600
	Intensity of sea breeze ( $\text{ms}^{-1}$ )	3.4	3.5	5	3.9	5	4

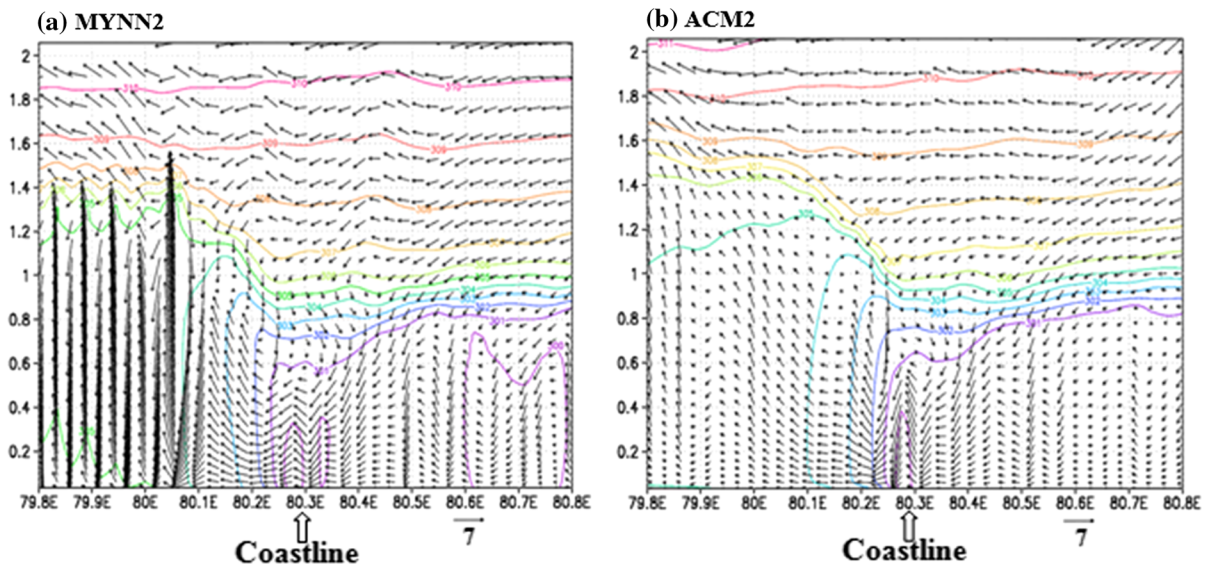


Figure 8

Vertical cross section of simulated wind vector ( $U$  and  $W$  components) and potential temperature from inner most domain (d03) at latitude ( $13^{\circ}\text{N}$ ) across Chennai for five different PBL schemes at 0700 UTC on 13 April 2011 for pre-monsoon case; the  $W$  component has been multiplied by a factor of 50; contour interval for potential temperature is 1 K

distribution are evident in all the simulations. The potential temperature distribution indicates stable stratification from  $\sim 600\text{-m}$  level over the sea area and  $\sim 1500\text{ m}$  over the land area indicating the gradual decrease of boundary layer height near the coast. A parabolic mixed layer with progressively increasing height is noticed across the coast (Fig. 8). The sharp variation of potential temperature at the coast indicates formation of TIBL due to mixing of cool and humid marine air mass with the warm and dry continental air mass. The vertical extent of this TIBL simulated as about  $200\text{--}250\text{ m}$  in QNSE, MYJ, YSU, and MYNN2 and as about  $400\text{ m}$  in ACM2. The simulated circulation across the coast in all PBL cases shows a low-level land ward flow below  $800\text{-m}$  height from the sea and a return flow from the land to sea at about  $1200\text{-m}$  height. The location of the return flow is about  $20\text{ km}$  from the coastline. The zone of horizontal flow convergence called sea-breeze front over land area is associated with vertical motion. The sea-breeze front has relatively strong vertical velocities ( $0.2\text{--}0.4\text{ ms}^{-1}$ ) over the land areas (not shown) in the simulations during the pre-monsoon case as compared to winter case. The TKE-based turbulence closures (QNSE, MYNN2, and MYJ) produced stronger vertical winds (figure not shown). These

differences in boundary layer between winter and pre-monsoon would have different consequences. In winter due to stable stratification, the pollution distribution would be confined to the lower  $1.2\text{ km}$  uniformly across the coast, as found in Madala et al. (2016). However, in pre-monsoon, the pollution concentrations due to sources along the coast would be dispersing less near the coast due to shallow PBL, which leads to fumigation conditions

### 3.3. Simulation of Surface Meteorological Variables

Here, the low-level WS ( $\text{ms}^{-1}$ ), WD ( $^{\circ}$ ), AT ( $^{\circ}\text{C}$ ), and RH (%) that influence the atmospheric dispersion (Seaman 2000) are compared with the in situ observations at hourly intervals at the Sathyabama university station, Chennai. The diurnal variation of AT, RH, WS, and WD with different PBL schemes over 2 days for each season along with the available observations is presented in Figs. 9 and 10.

From the model simulations and observations, it is seen that the air temperatures in Chennai city (Fig. 9) show small diurnal range ( $4.0\text{ }^{\circ}\text{C}$ ) in winter case and relatively, large diurnal range ( $\sim 10\text{ }^{\circ}\text{C}$ ) in pre-monsoon, monsoon, and post-monsoon cases thus suggesting larger daytime heating and convective

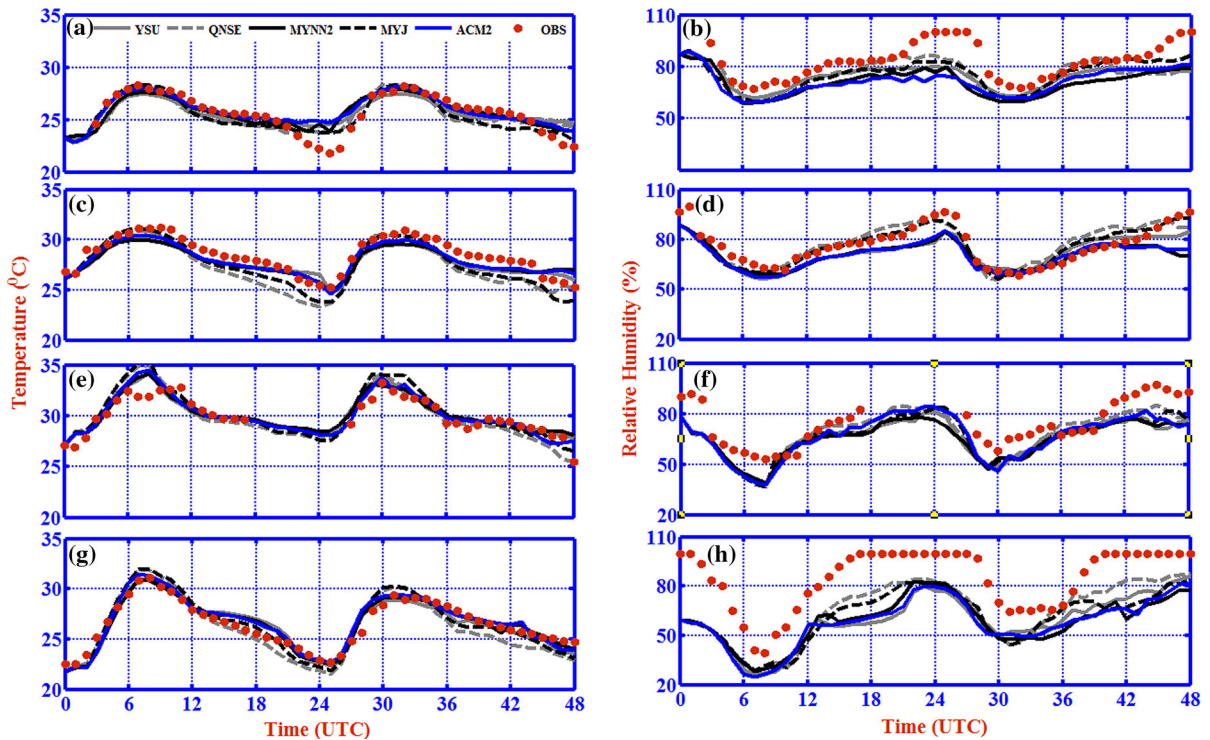


Figure 9

Comparison of model simulations of surface meteorological parameters **a, c, e, g** temperature ( $^{\circ}\text{C}$ ) and **b, d, f, h** relative humidity (%) over Sathyabama University during 27–29 January 2011 for winter season (**a, b**), 06–08 April 2011 for pre-monsoon season (**c, d**), 14–16 August 2011 for monsoon season (**e, f**) and 09–11 November 2011 for post-monsoon season (**g, h**)

mixing of air pollution in the latter cases. The lowest air temperatures are found during January (winter season) and the highest temperatures during August (monsoon) which could be due to dry weather in monsoon season over Chennai and continuation of pre-monsoon time heating in this region (Rao 1976). The tower situated in Sathyabama University site is about 25 km away from the coast and experiences pre-monsoon sea breeze in the daytime. It has been found that both observed and model simulated air temperatures during the pre-monsoon are moderate because of development of mesoscale sea breezes, which augment the PBL temperatures by advection of cool and humid air mass from marine region. The qualitative comparisons indicate that QNSE and MYJ PBL schemes have warm bias in night temperatures, while ACM2, MYNN2, and YSU produced good comparisons. The simulations show that the diurnal range in RH over Chennai is relatively high in post-monsoon season and winter season relative to the pre-monsoon season and monsoon season. A dry bias in

the RH is noted in the simulations with QNSE and MYJ PBL schemes, whereas ACM2, MYNN2, and YSU showed close agreement with observations. Overall, both air temperature and relative humidity better simulated in ACM2, MYNN2, and YSU compared to other PBL schemes.

It is noticed that in all the simulations, WS is overestimated in most of the seasons and close comparisons are obtained in post-monsoon season (Fig. 10). The winds simulated with MYNN2, YSU, and ACM2 are in better agreement with observations, whereas QNSE and MYJ produced stronger winds. All the PBL schemes simulated, the wind direction well in most seasonal cases, though QNSE and MYJ performed slightly better in winter season. Results indicate that the pre-monsoon case has largest duration ( $\approx 12$  h) of sea breeze (Fig. 10d) followed by monsoon ( $\sim 6$  h) (Fig. 10f) and post-monsoon ( $\sim 3$  h) (Fig. 10f) cases. In the wintertime, the sea breeze is not discernible from strong northeasterly synoptic winds (Fig. 10b; Table 1).

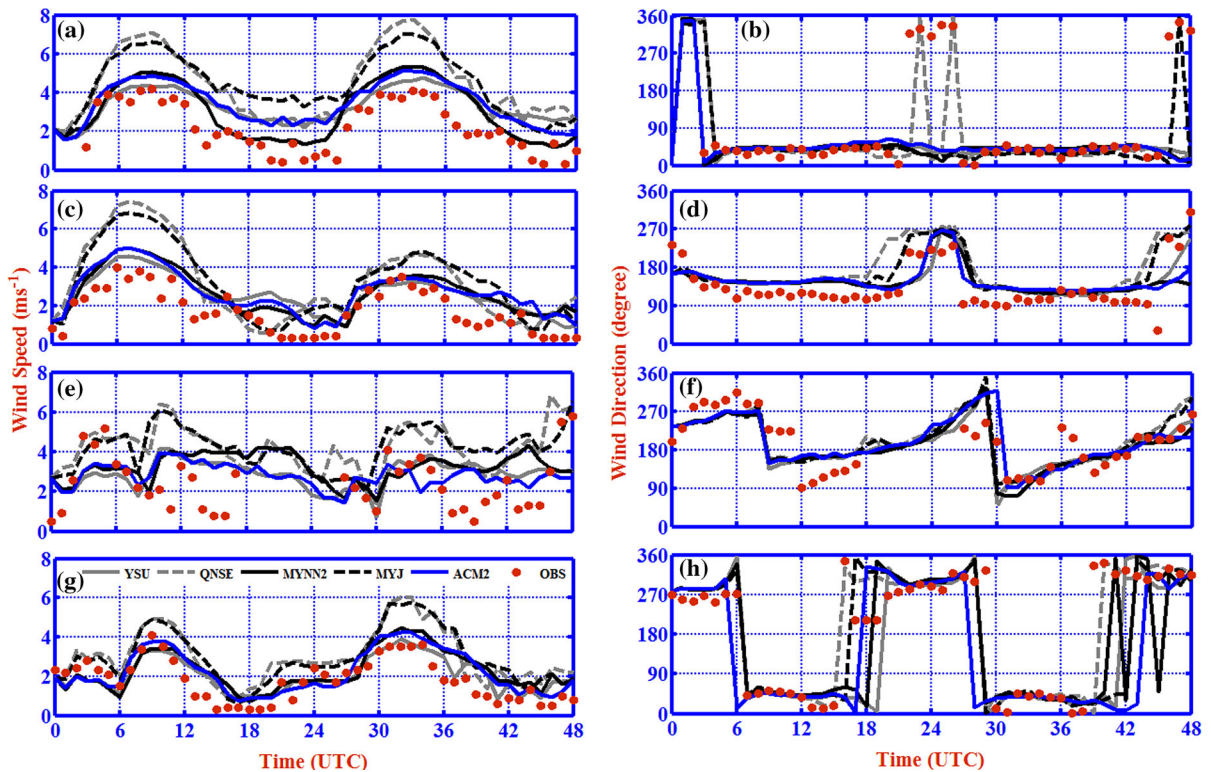


Figure 10

Comparison of model simulations of surface meteorological parameters **a, c, e, g** wind speed ( $\text{ms}^{-1}$ ) and **b, d, f, h** wind direction ( $^{\circ}$ ) (%) over Sathyabama University during 27–29 January 2011 for winter season (**a, b**), 06–08 April 2011 for pre-monsoon season (**c, d**), 14–16 August 2011 for monsoon season (**e, f**), and 09–11 November 2011 for post-monsoon season (**g, h**)

### 3.4. Thermo-dynamical Structure of the PBL

The thermo-dynamical state of PBL plays an important role in mixing and dispersion of air pollutants by controlling the boundary layer stability. While deep-mixed layers enhance the dispersion, shallow mixed layers restrict the vertical diffusion of pollutants thus promoting the chance of choking (Cimorelli et al. 2004; Rahul et al. 2015). The thermo-dynamical structure of the simulated PBL is analyzed from vertical profiles of equivalent potential temperature, RH, WS, and WD and compared with radiosonde data. Profiles from simulations are inter-compared at 0000 UTC (0530 IST) (along with observations) and 0600 UTC (1130 IST) (without observations) on 28 January 2011 (winter case) (Fig. 11), 07 April 2011 (pre-monsoon case) (Fig. 12), 15 August 2011 (monsoon case) (figure not shown), and 10 November 2011 (post-monsoon case) (figure not shown). The vertical variation of equivalent potential temperature in the winter case

indicates inversion layers up to 300-m AGL, neutral atmosphere up to 900-m AGL, and slight unstable layers up to 1500 m. All the PBL schemes simulated these features. Especially, the surface inversion layers are well-simulated by YSU, ACM2, MYNN2, and MYJ schemes (Fig. 11d). The vertical variations are well-simulated with YSU, ACM2, and QNSE for WS, YSU, QNSE, and MYNN2 for WD, and YSU, MYNN2, and ACM2 for RH. The increasing WS, WD shear, and decreasing relative humidity all indicate stable atmosphere in the winter morning conditions and all five PBL schemes performed well to reproduce these characteristics. The daytime profiles at 0600 UTC (1130 IST) from simulations show uniform WS with steady direction, increasing humidity and uniform potential temperature up to a height of about 900 m indicating formation of convective mixed boundary layer. Similar vertical structure is simulated in pre-monsoon case in the morning time (Fig. 12d) indicating



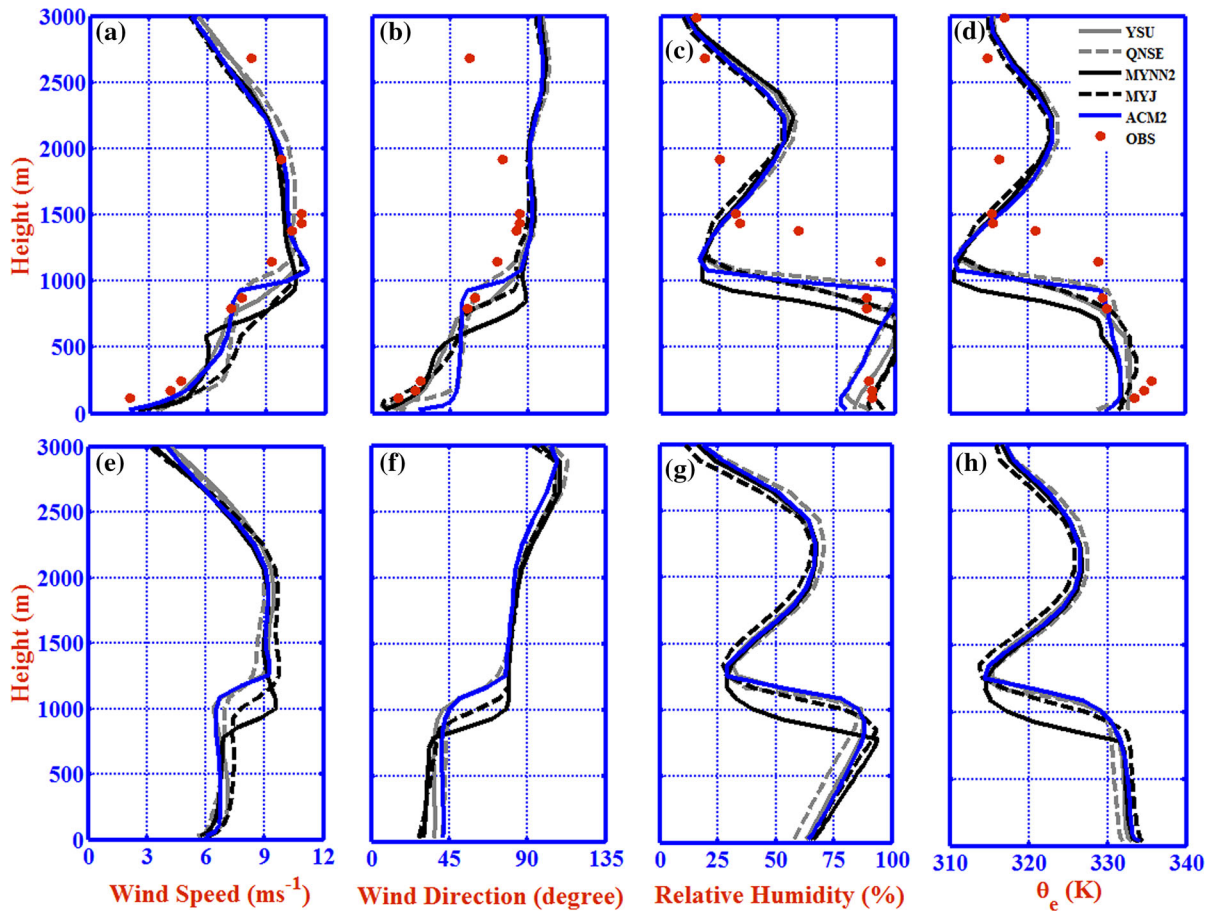


Figure 11

Comparison of model simulated profiles of **a, e** wind speed ( $\text{ms}^{-1}$ ), **b, f** wind direction ( $^{\circ}$ ), **c, g** relative humidity (%), and **d, h** equivalent potential temperature ( $\theta_e$ ) (K) with radiosonde observations over Chennai on 28 January 2011 (winter case) at 0000 UTC with observations and 0600 UTC

inversion condition in the surface layer and stable atmospheric condition up to 1 km AGL, though with slightly stronger winds compared to winter. These stable morning conditions in both winter and pre-monsoon cases would confine the pollutant plumes in the lower regions and lead to poor air quality (Panda et al. 2009). However, the daytime unstable mixed layer extended up to 1.2 AGL in summer. Thus, the vertical profiles in different seasons indicate that in general, YSU, ACM2, and QNSE produce deep-mixed layers and give strong diffusion, whereas MYJ and MYNN2 produce relatively shallow mixed layers and produce less dispersion (Madala et al. 2016). Thus, overall, the ARW model well-simulated the PBL structure and its vertical variation reasonably well in all seasons.

### 3.5. Error Statistics of Surface Meteorological Variables

The error statistics (Table 2) for surface meteorological variables (AT, RH, WS, U, and V winds) indicate that YSU scheme followed by MYNN2 and ACM2 produces better simulations with least errors and higher correlation for air temperature. For relative humidity, QNSE scheme followed by MYJ and ACM2 produced lesser errors and higher correlation. For wind speed, the simulation with ACM2 scheme followed by MYNN2 and YSU produced least errors and better correlations. Both  $U$  and  $V$  components better simulated with ACM2 scheme followed by MYNN2 and YSU (Table 2) indicating good simulation of wind direction



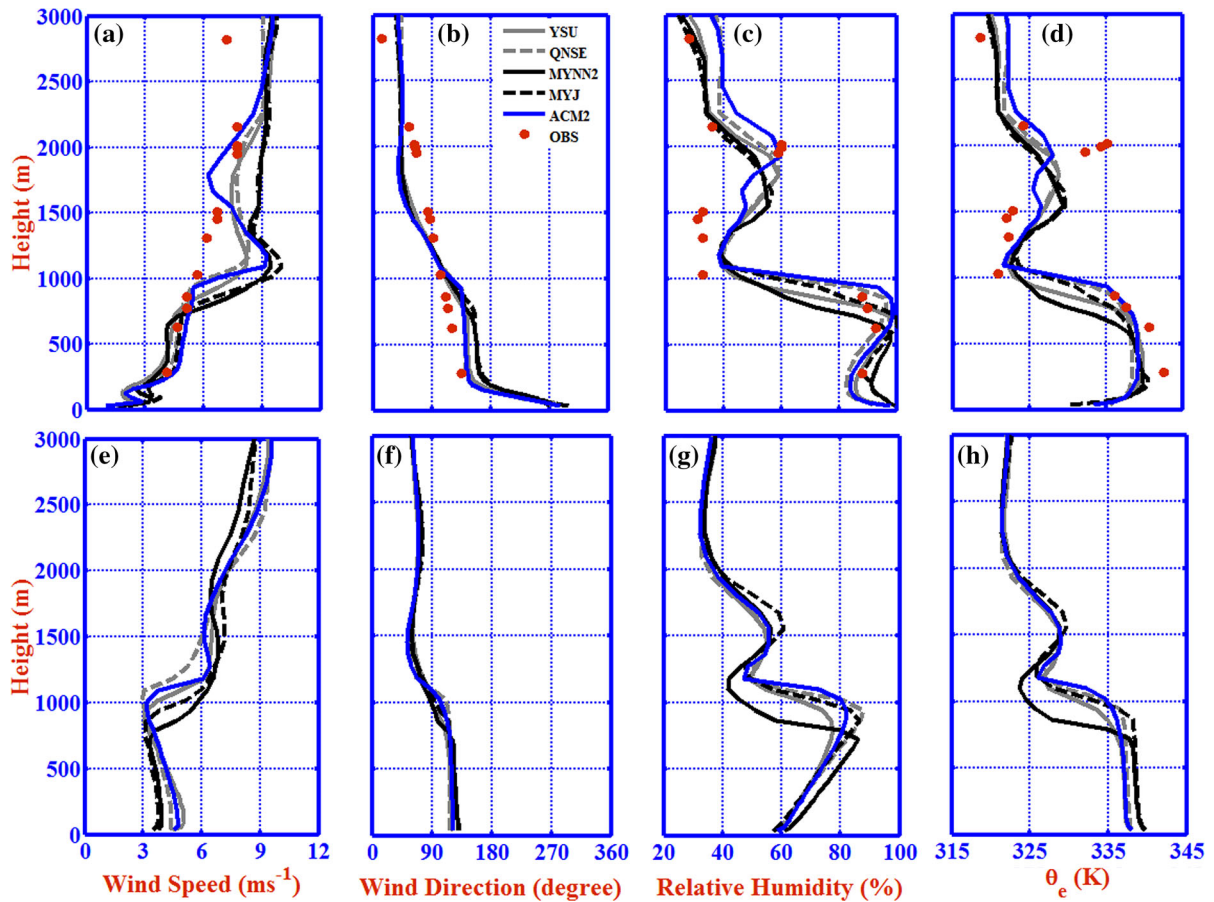


Figure 12

Comparison of model simulated profiles of **a, e** wind speed ( $\text{ms}^{-1}$ ), **b, f** wind direction ( $^{\circ}$ ), **c, g** relative humidity (%), and **d, h** equivalent potential temperature ( $\theta_e$ ) (K) with radiosonde observations over Chennai on 07 April 2011 (pre-monsoon case) at 0000 UTC with observations and 0600 UTC

compared to other PBL schemes. Thus, considering different variables, the model PBL physics ACM2 followed by MYNN2 and YSU produced better comparisons for the dynamical and thermo-dynamical variables in the boundary layer indicating their suitability for wind field simulations required in air quality studies in this region.

#### 4. Conclusions

The local meteorology plays a crucial role in air pollution transport and dispersion in coastal cities. In this work, the meteorological flows in the coastal metropolitan city of Chennai, south India are simulated using the ARW mesoscale model to examine

their characteristics over typical representative days in different seasons and validated with observations. Simulations revealed diurnal variation in the boundary layer flows due to the occurrence of land-sea breeze circulations over Chennai in different seasons. Results show that the characteristics of local flows vary in different seasons due to variation in the synoptic flow. Simulations revealed that the sea-breeze circulation is pre-dominant during pre-monsoon season prevailing for nearly 12 h in the day and less frequent ( $\sim 6$  h) in the monsoon and post-monsoon ( $\sim 3$  h) seasons. This implies that the re-circulation phenomena leading to local air pollution episodes would be pre-dominant in the pre-monsoon cases compared to the monsoon and post-monsoon cases. Simulations revealed that the sea breeze, which

Table 2

Error statistics for simulated air temperature, relative humidity, wind speed, and vector winds

Parameter	Errors	YSU	QNSE	MYNN2	MYJ	ACM2
Air temperature (°C)	MB	-0.62	-1.40	-0.90	-1.35	-0.91
	MAE	1.40	1.77	1.50	1.68	1.52
	RMSE	1.73	2.11	1.81	2.02	1.86
	CC	0.90	0.91	0.91	0.92	0.90
Relative humidity (%)	MB	-4.91	0.54	-5.04	0.86	-4.05
	MAE	9.57	8.98	8.97	8.80	8.91
	RMSE	12.50	11.34	11.73	11.25	11.60
	CC	0.70	0.71	0.74	0.73	0.73
Wind speed (ms <sup>-1</sup> )	MB	1.16	1.73	0.91	1.77	0.84
	MAE	1.41	1.89	1.27	1.92	1.18
	RMSE	1.71	2.25	1.56	2.28	1.44
	CC	0.67	0.69	0.71	0.70	0.75
U wind (ms <sup>-1</sup> )	MB	-0.01	-0.37	-0.15	-0.34	-0.20
	MAE	1.52	1.81	1.39	1.76	1.21
	RMSE	2.02	2.27	1.81	2.22	1.59
	CC	0.77	0.79	0.79	0.80	0.80
V wind (ms <sup>-1</sup> )	MB	0.28	0.22	0.21	0.34	0.26
	MAE	1.48	1.84	1.40	1.89	1.44
	RMSE	2.08	2.53	2.06	2.56	2.14
	CC	0.67	0.65	0.66	0.66	0.66

modifies the boundary layer near the coast, influences the flow field over Chennai in pre-monsoon and monsoon seasons. The TIBL height at the coast is simulated as 200–250 m in different simulations during pre-monsoon. The horizontal and vertical extents of sea-breeze flow are about 60 km and 900 m, respectively, in pre-monsoon and monsoon cases, which cover nearly 60% of the year. In the winter season, the model simulations show that the synoptic wind dominates the boundary layer flow and sea breeze is not well-defined except for a small change in the wind direction. The ARW model could simulate the diurnal variation in various meteorological variables and the vertical boundary layer structure in good agreement with observations.

The sensitivity experiments with five different PBL physics schemes revealed that the ACM2 followed by MYNN2 and YSU produced various boundary layer meteorological variables in close agreement with observations, although the winds are little over-predicted with all the options corroborating the previous studies at southeast coast (Hariprasad et al. 2014). The differences in the simulated flow field with different PBL parameterizations are due to differences in eddy diffusivities, which are computed

variously in different schemes. The better performance of ACM2 and MYNN2 over other schemes is due to better representing the mixing under stable as well as convective conditions. The DWR observations employed in the present study helped to compare the simulated flow fields vertically and temporally and thus provided a more robust validation. The model outputs with these PBL physics options find application in understanding airflow trajectories, source regions and to assess the air quality due to various industrial and vehicular pollutants.

### Acknowledgements

Authors acknowledge the Cyclone Detection Radar (CDR) Station, Indian Meteorological Department (IMD), Chennai, India for providing Doppler Weather Radar (DWR) wind data. We acknowledge the Indian Space Research Organization (ISRO) for providing automated weather stations data. Mr. Sardar Maran, Sathyabama University acknowledged for providing the meteorological tower observations. The first author would like to thank Dr. B. Venkatraman (Division Head and Associate Director, RSEG/IGCAR) and Dr. R. Baskaran (Head, RIAS) for providing the facilities to carry out this research work at IGCAR for Ph.D. The first author also gratefully acknowledges Indian Institute of Technology Kharagpur for providing research fellowship and necessary facilities to conduct PhD work. Authors thank anonymous reviewers for their technical comments and suggestions, which helped to improve the manuscript.

### REFERENCES

- Bouchlaghem, K., Ben Mansour, F. B., & Elouragini, S. (2007). Impact of a sea breeze event on air pollution at the Eastern Tunisian Coast. *Atmospheric Research*, 86, 162–172.
- Cimorelli, A. J., Perry, G. S., Venkatram, A., Weil, J. C., Paine, R. J., Wilson, R. B., et al. (2004). AERMOD: A dispersion model for industrial source applications. Part 1: General model formulation and boundary layer characterization. *Journal of Applied Meteorology*, 44, 682–693.
- Goyal, P., & Rama Krishna, T. V. B. P. S. (2002). Dispersion of pollutants in convective low wind: a case study of Delhi. *Atmospheric Environment*, 36, 2071–2079.

- Gryning, S. E., & Batchvarova, E. (1990). Analytical model for growth of the coastal internal boundary layer during onshore flow. *Quarterly Journal Royal Meteorological Society*, *116*, 187–203.
- Hariprasad, K. B. R. R., Srinivas, C. V., Bagavath Singh, A., Vijaya Bhaskara Rao, S., Baskaran, R., & Venkatraman, B. (2014). Numerical simulation and intercomparison of boundary layer structure with different PBL schemes in WRF using experimental observations at a tropical site. *Atmospheric Research*, *145*, 27–44.
- Jayanthi, V., & Krishnamoorthy, R. (2006). Key airborne pollutants—Impact on human health in Manali, Chennai. *Current Science*, *90*(3), 405–413.
- Joseph, B., Bhatt, B. C., Koh, T. Y., & Chen, S. (2008). Sea breeze simulation over the Malay Peninsula in an intermonsoon period. *Journal of Geophysical Research*, *113*, D20122. doi:10.1029/2008JD010319.
- Lasry, F., Coll, I., & Buisson, E. (2005). An insight into the formation of severe ozone episodes: modelling the 21/03/01 event in the ESCOMPTE region. *Atmospheric Research*, *74*(1–4), 191–215.
- Li, X. X., Koh, T. Y., Entekhabi, D., Roth, M., Panda, J., & Norford, L. K. (2013). A multi-resolution ensemble study of a tropical urban environment and its interactions with the background regional atmosphere. *Journal of Geophysical Research: Atmospheres*, *118*, 9804–9818. doi:10.1002/jgrd.50795.
- Liu, H., & Chan, J. C. L. (2002). An investigation of air-pollutant patterns under sea–land breezes during a severe air-pollution episode in Hong Kong. *Atmospheric Environment*, *36*, 591–601.
- Luhar, A. K., & Hurley, P. J. (2003). Application of a prognostic model TAPM to sea-breeze flows, surface concentrations, and fumigating plumes. *Environmental Modelling and Software*, *19*, 591–601.
- Madala, S., Satyanarayana, A. N. V., & Narayana Rao, T. (2014). Performance evaluation of PBL and cumulus parameterization schemes of WRF ARW model in simulating severe thunderstorm events over Gadanki MST radar facility—Case study. *Atmospheric Research*, *139*, 1–17.
- Madala, S., Satyanarayana, A. N. V., & Srinivas, C. V. (2015a). Simulation of atmospheric dispersion of NO<sub>x</sub> over complex terrain region of Ranchi with FLEXPART-WRF by incorporation of improved turbulence intensity relationships. *Atmospheric Environment*, *123*, 139–155.
- Madala, S., Satyanarayana, A. N. V., Srinivas, C. V., & Kumar, M. (2015b). Mesoscale atmospheric flow-field simulations for air quality modelling over complex terrain region of Ranchi in eastern India using WRF. *Atmospheric Environment*, *107*, 315–328.
- Madala, S., Srinivas, C. V., Hariprasad, K. B. R. R., & Satyanarayana, A. N. V. (2016). Air quality simulation of NO<sub>x</sub> over the tropical coastal city Chennai in Southern India with FLEXPART-WRF. *Atmospheric Environment*. doi:10.1016/j.atmosenv.2015.12.052.
- Mahrer, Y., & Pielke, R. A. (1977). The effects of topography on the sea and land breezes in a two-dimensional numerical model. *Monthly Weather Review*, *105*, 1151–1162.
- Melas, D., Ziomas, I. C., & Zerefos, C. S. (1995). Boundary layer dynamics in an urban coastal environment under sea breeze conditions. *Atmospheric Environment*, *29*(24), 3605–3617.
- Ohashi, Y., & Kida, H. (2002). Local circulations developed in the vicinity of both coastal and inland urban areas: Numerical study with a mesoscale atmospheric model. *Journal of Applied Meteorology*, *41*, 30–45.
- Panda, J., & Sharan, M. (2012). Influence of land-surface and turbulent parameterization schemes on regional-scale boundary layer characteristics over northern India. *Atmospheric Research*, *112*, 89–111.
- Panda, J., Sharan, M., & Gopalakrishnan, S. G. (2009). Regional scale boundary layer characteristics over northern India with special reference to the role of Thar Desert in regional scale transport. *Journal of Applied Meteorology and Climatology*, *48*, 2377–2402.
- Perez, C., Jimenez, P., Jorba, O., Sicard, M., & Baldasano, J. M. (2006). Influence of the PBL scheme on high-resolution photochemical simulations in an urban coastal area over the Western Mediterranean. *Atmospheric Environment*, *40*, 5274–5297.
- Prabha, T. V., Venkatesan, R., Radlgruber, E. M., Rengarajan, G., & Jayanthi, N. (2002). Thermal internal boundary layer characteristics at a tropical coastal site as observed by a mini-SODAR under varying synoptic conditions. *Journal of Earth System Science*, *111*, 63–77.
- Prtenjak, M. T., & Grisogono, B. (2002). Idealised numerical simulations of diurnal sea breeze characteristics over a step change in roughness. *Meteorologische Zeitschrift*, *11*, 345–360.
- Rahul, B., Satyanarayana, A. N. V., Rama Krishna, T. V. B. P. S., & Madala, S. (2015). Sensitivity of PBL parameterization schemes of Weather Research Forecasting Model and coupling with AERMOD in the dispersion of NO<sub>x</sub> over Visakhapatnam (India). *Asia-Pacific Journal of Chemical Engineering*, *10*(3), 356–368.
- Rao, Y. P. (1976). *Southwest monsoon. Vol. 1 Meteorological monograph: synoptic meteorology*, No. 1/1976. New Delhi: India Meteorological Department.
- Reche, C., Viana, M., Moreno, T., Querol, X., Alastuey, A., Pey, J., et al. (2011). Peculiarities in atmospheric particle number and size-resolved speciation in an urban area in the western Mediterranean: results from the DAURE campaign. *Atmospheric Environment*, *45*, 5282–5293.
- Ruscher, P., Gould, K., Korotky, J., & Hagemeyer, B. (1995). *Doppler weather radar studies of the florida sea breeze and associated mesoscale flow systems*. 14th Conference, Weather Analysis and Forecasting, Amer. Meteorol. Soc. Dallas, TX. pp. 343–346.
- Seaman, N. L. (2000). Meteorological modeling for air-quality assessments. *Atmospheric Environment*, *34*, 2231–2259.
- Sharan, M., Yadav, A. K., Singh, M. P., Agarwal, P., & Nigam, S. (1995). A mathematical model for the dispersion of air pollutants in low wind conditions. *Atmospheric Environment*, *30*(8), 1209–1220.
- Shin, H. H., & Hong, S. Y. (2011). Intercomparison of planetary boundary-layer parameterizations in the WRF model for a single day from CASES-99. *Boundary-Layer Meteorology*, *139*, 261–281.
- Simpson, M., Warrior, H., Raman, S., Aswathanarayana, P. A., Mohanty, U. C., & Suresh, R. (2007). Sea-breeze-initiated rainfall over the east coast of India during the Indian southwest monsoon. *Natural Hazards*. doi:10.1007/s11069-006-9081-2.
- Skamarock, W. C., Klemp, J. B., Dudhia, J., Gill, D. O., Barker, D. M., Dudhia, M. G., Huang, X., Wang, W., & Powers, Y. (2008). *A description of the Advanced Research WRF Ver.30*. NCAR technical note. NCAR/TN-475STR. Meso-scale and Micro-scale

- Meteorology Davison, National Centre for Atmospheric Research, Boulder Colorado, USA.
- Srimuruganandam, B., & Shiva Nagendra, S. M. (2011). Characteristics of particulate matter and heterogeneous traffic in the urban area of India. *Atmospheric Environment*, *45*, 3091–3102.
- Srinivas, C. V., Hariprasad, K. B. R. R., Naidu, C. V., Baskaran, R., & Venkatraman, B. (2015). Sensitivity analysis of atmospheric dispersion simulations by FLEXPART to the WRF simulated meteorological predictions in a coastal environment. *Pure and Applied Geophysics*. doi:10.1007/s00024-015-1104-z.
- Srinivas, C. V., Venkatesan, R., & Bagavath Singh, A. (2005). A numerical study of the influence of synoptic flow on coastal mesoscale circulations on the East and West coast of India. *Mausam*, *56*(1), 73–82.
- Srinivas, C. V., Venkatesan, R., & Bagavath Singh, A. (2007). Sensitivity of mesoscale simulations of land–sea breeze to boundary layer turbulence parameterization. *Atmospheric Environment*, *41*, 2534–2548.
- Srinivas, C. V., Venkatesan, R., Somayaji, K. M., & Bagavath Singh, A. (2006). A numerical study of sea breeze circulation observed at a tropical site Kalpakkam on the east coast of India, under different synoptic flow situations. *Journal of Earth System Science*, *115*(5), 557–574.
- Suresh, R. (2007). Observation of sea breeze front and its induced convection over Chennai in southern peninsular India using doppler weather radar. *Pure and Applied Geophysics*, *164*, 1511–1525.
- Thilagaraj, P., Ravinder, R., & Kesavan, R. (2014). A study on air pollution and its impact on human health in Chennai city. *IOSR Journal of Mechanical and Civil Engineering*, *4*, 1–5 (e-ISSN: 2278-1684, p-ISSN: 2320-334N).
- Venkatesan, R., Rajendran, M., & Dasgupta, S. (2009). Analysis and numerical simulation of the meteorological observations at a tropical coastal site Chennai in India. *Atmospheric Research*, *92*, 505–521.
- Xie, B., Fung, J. C. H., Chan, A., & Lau, A. (2012). Evaluation of nonlocal and local planetary boundary layer schemes in the WRF model. *Journal of Geophysical Research*, *117*, D12103.
- Yoshikado, H. (1994). Interaction of the sea breeze with the urban heat islands of different sizes and locations. *Journal of the Meteorological Society of Japan*, *72*, 139–142.

(Received October 31, 2016, revised August 12, 2017, accepted August 30, 2017, Published online September 5, 2017)